ELSEVIER

Journal of Structural Geology 28 (2006) 654–668

JOURNAL OF STRUCTURAL GEOLOGY

www.elsevier.com/locate/jsg

A remote sensing study of active folding and faulting in southern Kerman province, S.E. Iran

Richard Thomas Walker *

Department of Earth Sciences, University of Oxford, Oxford OX1 3DP, UK

Received 4 April 2005; received in revised form 22 December 2005; accepted 22 December 2005
Available online 3 March 2006

Abstract

Geomorphological observations reveal a major oblique fold-and-thrust belt in Kerman province, S.E. Iran. The active faults appear to link the Sabzevaran right-lateral strike-slip fault in southeast Iran to other strike-slip faults within the interior of the country and may provide the means of distributing right-lateral shear between the Zagros and Makran mountains over a wider region of central Iran. The Rafsanjan fault is manifest at the Earth's surface as right-lateral strike-slip fault scarps and folding in alluvial sediments. Height changes across the anticlines, and widespread incision of rivers, are likely to result from hanging-wall uplift above thrust faults at depth. Scarps in recent alluvium along the northern margins of the folds suggest that the thrusts reach the surface and are active at the present-day. The observations from Rafsanjan are used to identify similar late Quaternary faulting elsewhere in Kerman province near the towns of Mahan and Rayen. No instrumentally recorded destructive earthquakes have occurred in the study region and only one historical earthquake (Lalehzar, 1923) is recorded. In addition GPS studies show that present-day rates of deformation are low. However, fault structures in southern Kerman province do appear to be active in the late Quaternary and may be capable of producing destructive earthquakes in the future. This study shows how widely available remote sensing data can be used to provide information on the distribution of active faulting across large areas of deformation.

Keywords: Iran; Active tectonics; Active faults; Folding; Remote sensing

1. Introduction

This paper uses geomorphological observations to describe the growth of strike-slip and thrust faults in southern Kerman province, southeast Iran (Fig. 1). GPS studies across this part of Iran suggest low rates of deformation (e.g. Vernant et al., 2004a,b) and it is often considered to behave as a non-deforming block within the Arabia–Eurasia collision zone. The observations in this paper instead suggest that the region is important in the active tectonics of Iran and that the active faults of Southern Kerman province may provide the means of distributing the right-lateral shear between the Zagros Mountains and the Makran accretionary prism in southern Iran over a wider region of central Iran, by transferring right-lateral shear from the Sabzevaran fault to the southeast of the study area, to the Anar fault of central Iran (Fig. 1c).

The observations in this paper show how studies of the landscape using remote sensing data can provide information on the active tectonics of a region and the distribution of active faults, many of which may be unmapped. This approach is particularly relevant in areas such as eastern Iran, where routine fieldwork may be difficult and where very few details are available on structures developed within Quaternary deposits. Without such studies, the distribution of active faults, and the hazard posed by these faults, may be underestimated. The observations presented in this paper draw on previous studies of active faulting, in Iran and elsewhere, where the link between slip on faults and the development of landscape features has been investigated in detail.

In the following sections, I first describe the types of observations used to infer the presence of active faults (Section 3). I then examine the geomorphology of the region around the town of Rafsanjan, which was damaged by the 1923 Lalehzar earthquake (Section 4). I then use similar observations to identify further potentially active faults within adjacent parts of Kerman province (Sections 5 and 6). The observations from satellite imagery are supported by brief fieldwork in one locality. The resulting map of active faulting is then used to

* Tel.: +44 1865 272013.
E-mail address: richw@earth.ox.ac.uk.

0191-8141/$ - see front matter © 2006 Elsevier Ltd. All rights reserved.
doi:10.1016/j.jsg.2005.12.014

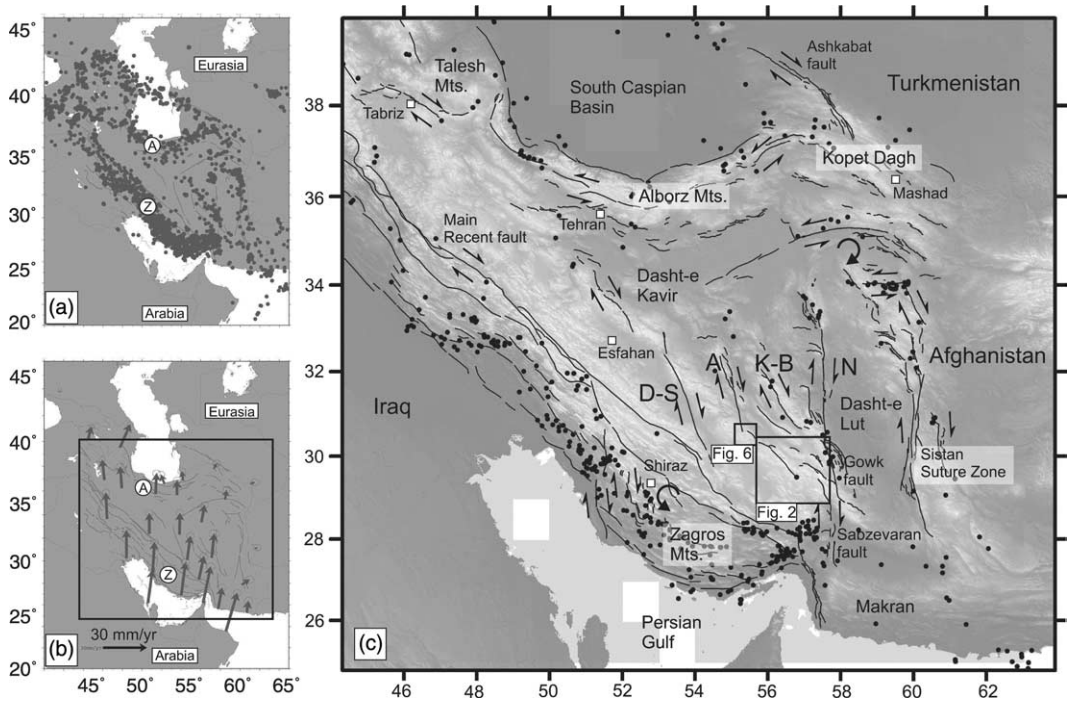

Fig. 1. (a) Instrumentally recorded earthquake epicentres in Iran from the catalogue of Engdahl et al. (1998). (b) A velocity field for Iran determined from repeated GPS measurements (Vernant et al., 2004a). Both the seismicity and the deformation measured by GPS are concentrated in the Zagros mountains (Z) in the south of the country and the Alborz mountains (A) in the north. Central parts of Iran (including the study region) are relatively aseismic and do not appear to be deforming rapidly at the present day. (c) Shaded SRTM topography of the study area showing the major active faults. Faults referred to in the text are named. Right-lateral strike-slip faults within central Iran are the Deh Shir fault (D-S), the Anar fault (A), the Kuh-Banan fault (K-B) and the Nayband fault (N), the latter of which forms the western margin of the Lut desert. The boxes represent regions shown in later figures. The map is in a mercator projection.

describe the role of the faults in the regional tectonics (Section 7).

2. Geological background

2.1. Active tectonics

The active tectonics of Iran are dominated by the northward motion of Arabia with respect to Eurasia (Fig. 1). At longitude 56°E, ~25 mm/yr of north–south shortening is accommodated across Iran (Sella et al., 2002; McClusky et al., 2003; Vernant et al., 2004a). Several large earthquakes have occurred on the right-lateral strike-slip fault systems along the western margin of the Dasht-e-Lut (Fig. 1; e.g. Berberian et al., 2001), which accommodate right-lateral shear between central parts of Iran and Afghanistan. However, low rates of seismicity lead the parts of central Iran west of the Dasht-e Lut desert (Fig. 1) to be considered as relatively strong and non-deforming crustal blocks, in which relatively few active faults have been mapped and relatively few historical earthquakes are recorded (Ambraseys and Melville, 1982). GPS velocities also suggest that the rates of deformation across central Iran are low, at ~3 mm/yr at the longitude of Tehran (Vernant et al., 2004a,b; see Fig. 1) and at rates of less than 2 mm/yr at the longitude of Kerman (Vernant et al., 2004b). The folds and faults described in this paper are situated in a part of Iran with little instrumentally recorded seismic activity (e.g. Figs. 1 and 2) and with few records of historical activity (e.g. Ambraseys and Melville, 1982), but as we shall see, there are clear indications of Quaternary fault movement. The faults described in this paper appear to link the right-lateral Sabzevaran fault in the south to the Anar right-lateral strike-slip fault in central Iran (Fig. 1) and hence play an important role in distributing the right-lateral shear between the Zagros and Makran mountains (Fig. 1) across central Iran.

2.2. Geology

The northwest–southeast-trending Kuh-e Bahr Aseman (~3800 m), Kuh Hezar (~4400 m), Kuh-e Lalehzar (~4350 m) and Kuh-e Mamzar (~3100 m) mountain ranges (Fig. 2) form part of the Sanandaj–Sirjan Tertiary volcanic belt, formed during closure of the Neo-Tethys and subduction of oceanic material (e.g. Stocklin, 1968). The Sanadaj–Sirjan ranges dominate the central part of the study area and separate regions of low relief. We call the northern region the Rafsanjan plain (with an average elevation of ~2000 m to the south of Kuh-e Kalleh Gav and 1600–1700 m to the north of Kuh-e Kalleh Gav) and the southern region the Sirjan plain, again with an elevation of roughly 1700 m (Fig. 2). Kuh-e Kalleh Gav and Kuh-e Jupar form isolated ranges within the Rafsanjan plain. Kuh-e Sekonj runs along the eastern boundary of the study area and borders the Gowk right-lateral strike-slip fault (Figs. 1 and 2; Berberian et al., 2001; Walker and Jackson, 2002). Kuh-e Sekonj and Kuh-e Jupar in the east of the study region consist of conformable Mesozoic and Tertiary

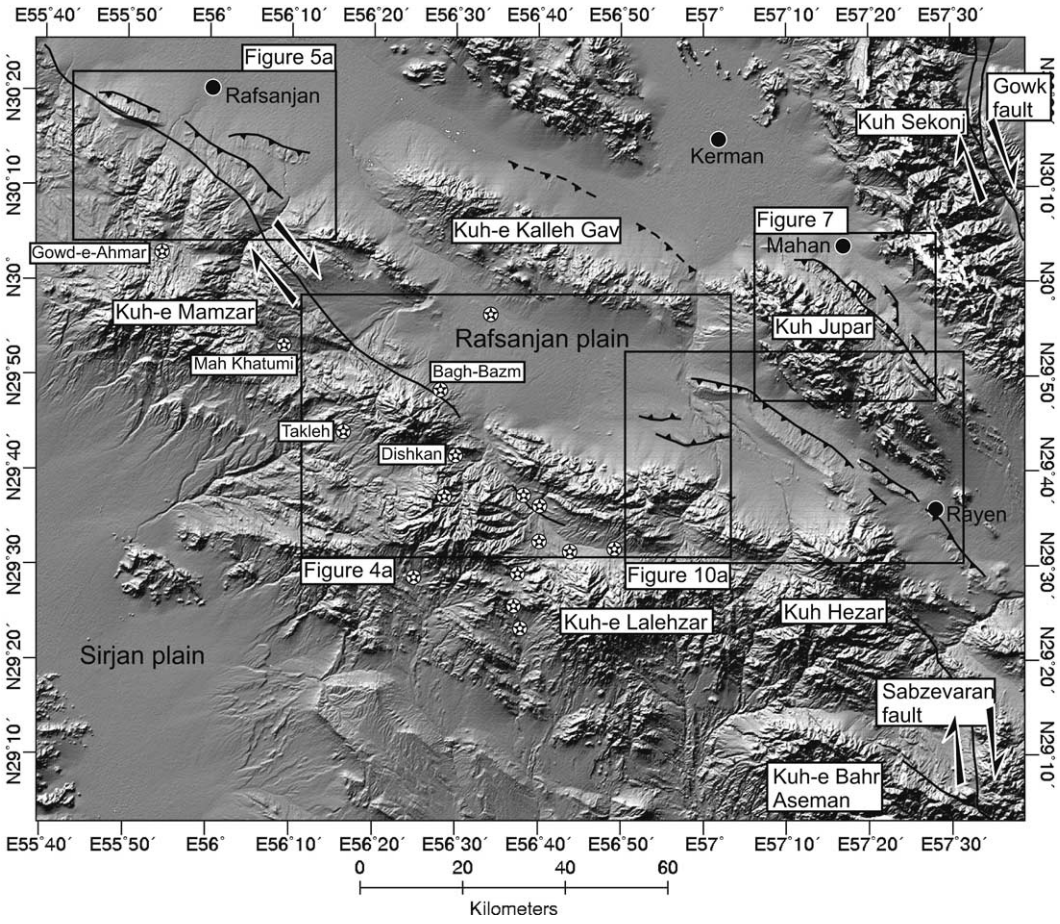

Fig. 2. Shaded SRTM topography of the study area showing the major population centres, topographic features and active faults. The boxes represent regions shown in later figures. Villages badly damaged or destroyed in the 1923 Lalehzar earthquake are labelled with circled stars. Damaged villages not covered by Fig. 4 are named here. This and all later maps are in a local zone UTM projection.

sediments. The bed-rock geology of northern parts of the Sanandaj–Sirjan zone (south of Anar and in the Kuh-e Kalleh Gav) form a sequence of Cretaceous and early Tertiary turbitide basins (Dimitrijevic, 1973). Rocks exposed within the high ranges of Kuh-e Lalehzar and Kuh-e Hezar are a mixture of unconformable Tertiary sediments and volcanic complexes, with up to 7 km thickness of Eocene volcanics exposed in Kuh-e Bahr Aseman massif (Dimitrijevic, 1973).

The Rafsanjan and Sirjan plains are underlain by thick deposits of Neogene and Quaternary sediment. The Neogene deposits are typically fine-grained and light-coloured marls and sandstones, which are likely to represent the sedimentation before the onset of uplift and faulting. The marls grade upwards into gravels shed from adjacent mountain ranges. The transition to gravel deposition probably marks the onset of active faulting in the region. The Neogene and Quaternary basin deposits have subsequently been deformed by folding. No detailed information exists on either the stratigraphy or structures developed in the Neogene and Quaternary deposits.

Large areas of eastern and central Iran are covered by large late Quaternary alluvial fan surfaces, which are often abandoned and incised by drainage. Although the patterns of river incision may be controlled at the local scale by fault movement (as seen in the examples described in later sections), the repeated cycles of deposition and incision within the river system must ultimately be driven by climatic variation within the late Quaternary, as is the case in other parts of central Asia (e.g. Brown et al., 1998; Van der Woerd et al., 2002; Pan et al., 2003). There is little chronological data to date periods of alluvial fan deposition in Iran. A recent study by Regard et al. (2005) dates two generations of regionally extensive alluvial fan deposits in southeast Iran at 5–9 ka and 13.6 ± 1.1 ka. A study by Fattahi et al. (in review) dates fan deposits at Sabzevar in northeast Iran at $\sim$9–13 ka. Whether the age of the fans in these two studies can be correlated to similar deposits elsewhere in Iran can only be shown by further work. However, the limited chronological data do appear to show that the most recent generations of alluvial fan deposition in Iran roughly date to $\sim$10 ka. The deformation and subsequent incision of Quaternary fan deposits can therefore be used to infer the presence of faults active in the late Quaternary and very possibly at the present-day.

3. Remote sensing observations of active faulting

The observations used in this paper to infer the presence of active faults are taken from the results of numerous studies, both within Iran and elsewhere, which have explored the link

between slip on active faults and the development of landscapes. In Iran, several recent studies of earthquakes show how indications of active faulting can be read from the local geomorphology (e.g. Berberian et al., 2000; Walker and Jackson, 2002; Walker et al., 2003, 2005; Hollingsworth et al., in review; Jackson et al., in review). Before introducing the examples described in this paper, it is worthwhile to first describe the types of observations that can be searched for in satellite imagery and digital topography in order to assess the potential for active strike-slip and thrust faulting. The relationships described below, and shown schematically in Fig. 3, are based on observations typically observed in regions of active thrust faulting and are not representative of any particular locality. The interpretation of landforms described in later sections should be read with reference to the following descriptions.

Strike-slip faults are common features in regions of continental deformation (e.g. Berberian et al., 2001; Van der Woerd et al., 2002; Regard et al., 2005). Late Quaternary activity on strike-slip faults can be determined from the lateral displacement of young landforms such as river terraces and alluvial fans, or from scarps introduced by slight dip-slip components of motion. The Bam earthquake of 2003 (e.g. Jackson et al., in review), showed the potential for strike-slip faults with low rates of slip and small dip-slip components to be undetectable in the geomorphology, due to their traces being removed by erosion (e.g. Talebian et al., 2004). Conversely, strike-slip faults within regions of bed-rock exposure may be obvious from their displacement of geological units, but present-day activity is difficult to determine unless the fault cuts through recent deposits, which might be rare in mountainous regions.

Thrust faults are commonly associated with folding (e.g. Lettis et al., 1997). Although discrete fault scarps are not always developed, movement on thrust faults during earthquakes does cause deformation at the Earth's surface (e.g. Stein and King, 1984; Stein and Yeats, 1989). Landforms generated from many repeated earthquakes result from the cumulative effect of uplift above the fault at depth (e.g. Jackson et al., 1996; Boudiaf et al., 1998; Keller et al., 1998, 1999). If slip on the thrust fault dissipates in the top few kilometres of the crust, or if the dip of the thrust steepens as it approaches the surface, it will cause folding of sediments on a comparable wavelength of a few kilometres (e.g. Stein and King, 1984). Fault-related folding is often developed away from mountainous regions and can often be identified in satellite imagery from the light-coloured Neogene marl deposits exposed in their cores.

Active thrust faults do not always reach the Earth's surface. Slip on these so-called 'blind' faults is instead accommodated as anticlinal folding in the top few kilometres of the crust (e.g. Fig. 3a; Stein and Yeats, 1989). Folds overlying 'blind' thrust faults typically develop steep asymmetric ridges on each limb with sharp erosional scarps on their inward-facing sides (e.g. the Tabas folds in NE Iran; Walker et al., 2003).

The ridges are formed of resistant gravels that do not erode as rapidly as the soft marls exposed in the fold cores. Young

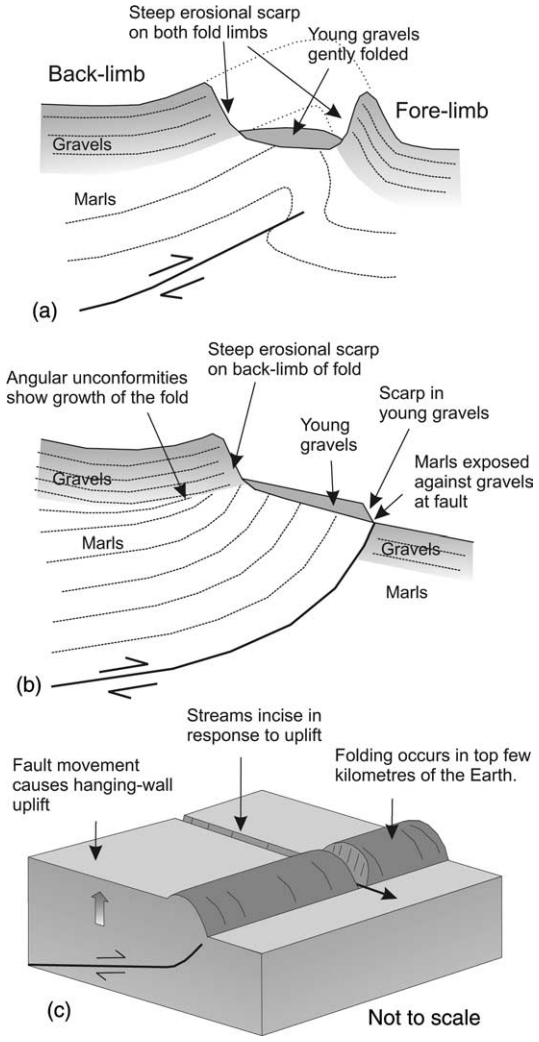

Fig. 3. (a) Schematic cross-section of a 'blind' thrust fault where slip on the fault is dissipated in the top few kilometres of the crust as anticlinal folding. Resistant gravel beds in the limbs of the fold form steep ridges with sharp inward-facing erosional scarps. The gravel ridges surround an area of low relief in the core of the fold where soft marl deposits have been eroded. Young gravel fans deposited across the fold are uplifted and warped, but do not show discrete scarps at the fore-limb margin of the fold. (b) Schematic cross-section of a thrust fault that reaches the Earth's surface. The fore-limb of the fold has been truncated, producing a sharp contact between highly tilted marl beds (on the hanging-wall) from undeformed gravel beds (on the footwall). Young gravel deposits have been displaced where they cross the fault forming a scarp. Growth of the fold during deposition of syn-faulting sediments results in angular unconformities (or growth) between bedding. (c) Block diagram showing the effect of dip on a thrust fault at depth. The hanging-wall block is uplifted with respect to the footwall, causing river incision over longer length-scales, but with much smaller amplitude than the incision through the fold itself.

alluvial surfaces deposited across the folds are uplifted and deformed across the anticline. However, as the main thrust does not reach the surface, discrete scarps are not developed in the alluvium at the margin of the fold. However, if the thrust does reach the Earth's surface (e.g. Fig. 3b), the fore-limb of the fold may be truncated and will lead to a sharp contact between folded Neogene marl deposits on the hanging-wall and undeformed gravel surfaces on the footwall (e.g. Fig. 3b).

A steep gravel ridge is only preserved on the back-limb of the fold and young alluvial surfaces show sharp scarps where they cross the fault.

Topography produced by long-term folding forms an obstacle that can affect local drainage (e.g. Burbank et al., 1996) and streams and rivers are often diverted around the ends of the fold. Remnants of the original drainage channels are sometimes preserved as 'dry valleys' within the anticlines, which show up as low-points, or 'wind-gaps', in the fold topography. Drainage deflections are often interpreted as the result of lateral increases in fold length (e.g. Jackson et al., 1996; Boudiaf et al., 1998; Keller et al., 1998, 1999), as fault-related folds must grow in length as slip is accumulated on the underlying fault (e.g. Cowie and Scholz, 1992). However, without information from detailed chronological studies it is difficult to confirm lateral propagation as a cause in any individual example.

Deep parts of non-horizontal thrust faults will also uplift overlying rocks, producing a hanging-wall uplift that is much broader than the folding caused by dissipation of slip, or steepening of the fault plane, in the top few kilometres of the Earth (e.g. Fig. 3c; Champel et al., 2002; Van der Beek et al., 2002). For instance, surface uplift resulting from aseismic slip on a blind thrust at Shahdad in eastern Iran was imaged by InSAR (Fielding et al., 2004). The uplift imaged by InSAR occurs over a much wider area than the narrow (2–4 km wide) anticlines obvious in the geomorphology (compare figs. 1 and 2 in Fielding et al. (2004)). Although the uplift due to folding in the top few kilometres of the crust will dominate the surface deformation (e.g. Fig. 3c), the broader-scale effects of uplift in the hanging-wall from repeated thrust fault movements has an identifiable influence not only on the topography but also on the patterns of drainage and drainage incision on a regional scale (e.g. Audemard, 1999; Benedetti et al., 2000; Walker et al., 2005). Alluvial rivers that have been blocked by fold topography can also introduce height changes between the hanging- and footwall blocks, by forced aggradation and ponding of sediment upstream of the back-limb of the fold (e.g. Burbank et al., 1996), which might then be incised by changes in the hydrology of the rivers. Care must therefore be taken to distinguish height changes (and stream incision) caused by tectonic uplift from changes introduced purely by sedimentation (which may be the case in the examples from Mahan, Section 5). Ideally, measurements of tectonic uplift of the hanging-wall should be taken from single fan surfaces that can be traced continuously across the fold and which would originally have had a roughly planar surface (as in Sections 4.3 and 6). Height changes across folds caused by hanging-wall uplift are particularly useful as an indicator of the presence of blind thrust faults, where discrete fault scarps are not seen at the Earth's surface.

In summary, regions of anticlinal folding in Iran can easily be identified from satellite imagery by the exposure of light-coloured Neogene marls exposed within their cores. The folding can be shown to be active by the presence of uplifted and incised late Quaternary gravel surfaces within the anticlines and sometimes by the diversion of drainage networks. The folds typically have a region of low relief in the core, where soft marls are exposed, which is surrounded by ridges of resistant folded gravel beds. If the thrust has propagated to the Earth's surface, it may truncate the fore-limb of the fold, placing highly tilted Neogene marls on the hanging-wall against flay-lying gravel beds on the footwall. Broader wavelength uplift of the hanging-wall of the fault can be seen in height changes across the fault and in asymmetric patterns of river incision.

4. Active folding and past earthquakes near Rafsanjan

In the following sections, I first describe the 1923 Lalehzar earthquake. Although the causative fault of the earthquake is not known, it is the only destructive event to be recorded within the study area, and hence demonstrates that despite the lack of instrumentally recorded seismicity there is a potential for earthquakes to occur in southern Kerman province. Later sections describe indications of late Quaternary faulting around the Rafsanjan region. Although some parts of the faults have been described before (e.g. Berberian, 1976), the observations provided here show that the fault system is part of a much larger zone of deformation than previously thought.

4.1. The 22 September 1923 Lalehzar earthquake

Rural areas southeast of Rafsanjan were damaged by a large earthquake occurring late at night on 22 September 1923 (e.g. Ambraseys and Melville, 1982). The epicentral region is within the Ab-e Lalehzar valley (Fig. 4a). The earthquake destroyed the villages of Lalehzar, Gughar, Khatib and Qaleh Askar (Ambraseys and Melville, 1982).

Berberian (1976) states that the destruction extended as far north as Dishkan, Bagh-Bazm and Gowd-e Ahmar (Figs. 2 and 4a), giving a much more elongate pattern of destruction. Roughly 200 people were killed. Lesser damage extended to Rafsanjan, Rayen and Kerman (Fig. 2). A large aftershock approximately 7 h after the main event caused further damage. Reports of heavy damage define an east–west to southeast–northwest elongate zone (e.g. Figs. 2 and 4a). The shape of this zone may not be evenly spread around the earthquake fault, as it may be influenced by an uneven distribution of population, with most villages situated within the main valley and tributaries of the Ab-e Lalehzar river (Fig. 4a).

4.2. The Rafsanjan strike-slip fault

The town of Rafsanjan is situated on alluvial apron deposits (elevation $\sim$1450 m) at the northern margin of the Kuh-e Mamzar mountains (elevations up to $\sim$3100 m). Berberian (1976) maps late Quaternary displacements along a northwest–southeast fault zone south of Rafsanjan (Fig. 2). The trace of the Rafsanjan fault is clear in both SRTM topography and ASTER satellite imagery (e.g. Figs. 4 and 5). Berberian (1976) calls this the Rafsanjan fault and describes it as $\sim$100 km long, with oblique right-lateral movement. At Kansabz village (Fig. 5b), he notes north-facing scarps $\sim$10 m high in

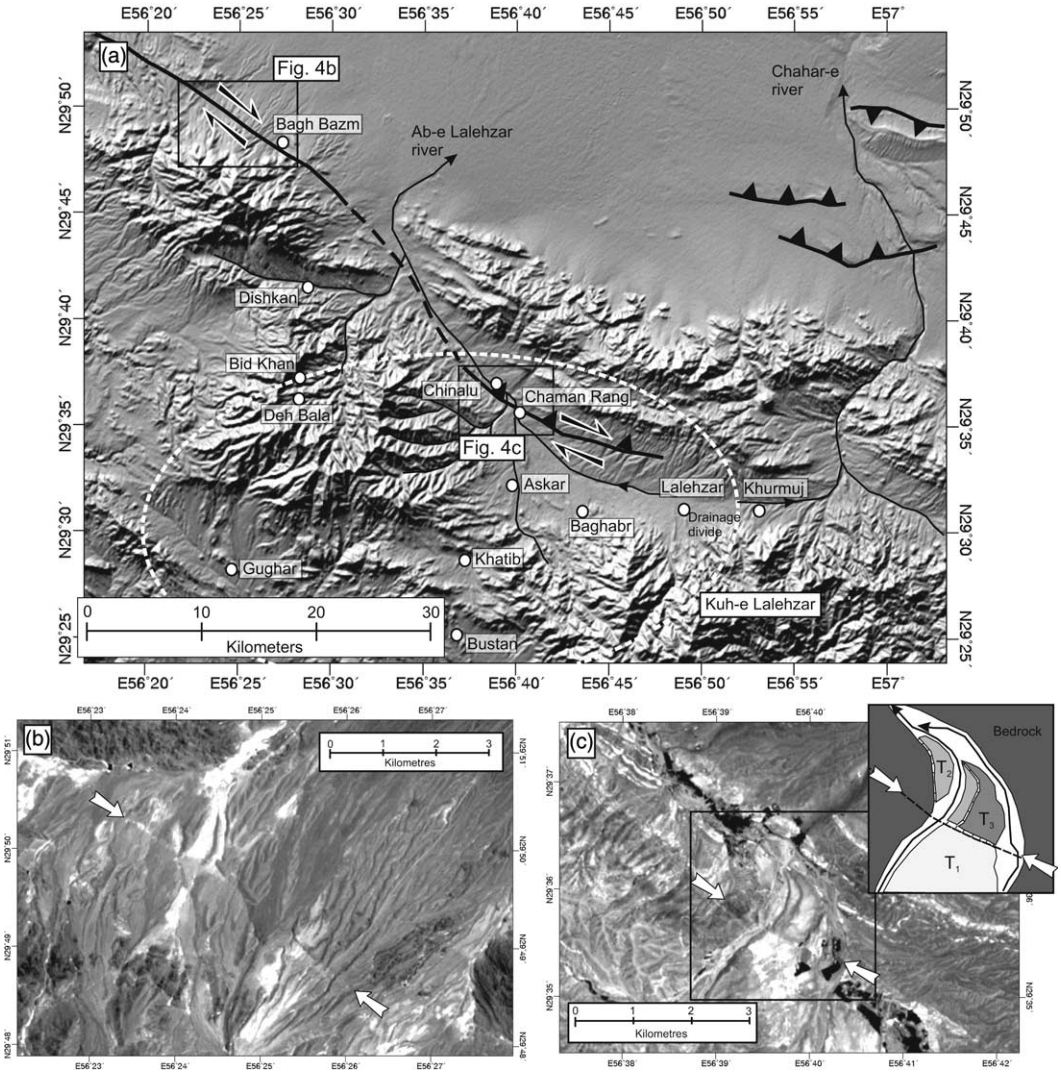

Fig. 4. (a) SRTM topography of the southeastern Rafsanjan fault and the epicentral region of the 22 September 1923 Lalehzar earthquake. Villages destroyed by the earthquake are labelled (Berberian, 1976; Ambraseys and Melville, 1982). The approximate limit of destruction given by Ambraseys and Melville (1982) is marked by the dotted white ellipse. Berberian (1976) gives a damage distribution that extends much further to the northwest, beyond Dishkan and Bagh-Bazm to Gowd-e-Ahmar (see Fig. 2). The Lalehzar valley is oriented east–west and separates the Kuh-e Lalehzar mountains from a lower parallel range to the north. Drainage west of ~56°50′E flows westwards into the Ab-e Lalehzar river. Waters east of ~56°50′E drain east into the Chahar-e river. Faults are shown as thickened black lines. The Lalehzar valley fault (in the centre of the image) is marked with thrust fault symbols to show the sense of vertical displacement. However, like the Rafsanjan fault to the northwest, it may also have a large component of strike-slip motion. The mapped fault segments have been linked by a dotted line. There is no direct evidence of Quaternary faulting along this inferred line in the satellite imagery. (b) ASTER image of alluvial fans cut by the Rafsanjan fault (marked by white arrows). (c) ASTER image of possible fault scarps (marked by white arrows) cutting across the floor of the Lalehzar river. The inset is a sketch of the faulting. T1–T3 are terrace levels, with T3 being the highest. The fault scarp is preserved on a river terrace situated between two active channels of the Ab-e Lalehzar river. The northern side appears to be uplifted, with two terrace levels, and incision of secondary drainage.

Quaternary alluvium. The water table appears to change in height across the fault at Kansabz, being ~10 m underground to the south of the fault trace, but deeper in qanats (man-made underground water tunnels used to transport water for irrigation and drinking) that are dug into gravels on the northern side of the fault only. The fault may form a barrier to the flow of water or may separate sediments of differing permeabilities. Berberian (1976) also states that some qanat tunnels have been dug along the fault trace itself, presumably to maximise the flow of water by tapping the elevated water table along the fault. The description of these qanats is very similar to those observed along the trace of the 1968 Dasht-e Bayaz earthquake ruptures in northeast Iran (e.g. Ambraseys and Tchalenko, 1969; Walker et al., 2004).

The Rafsanjan fault trace continues in alluvium northwestward to the margin of the Kuh-e Mosahem mountains (Fig. 6). The southern end of the north–south right-lateral Anar fault is also traced into the Kuh-e Mosahem mountains (Fig. 6). The Anar fault is likely to be active from its trace in Quaternary alluvium (Berberian, 1976; Walker and Jackson, 2004). The southern end of the Anar fault and the western end of the Rafsanjan fault are linked through the mountains by a narrow linear valley, which follows a geological fault (note the separation of lithologies across the valley in Fig. 6a). It appears

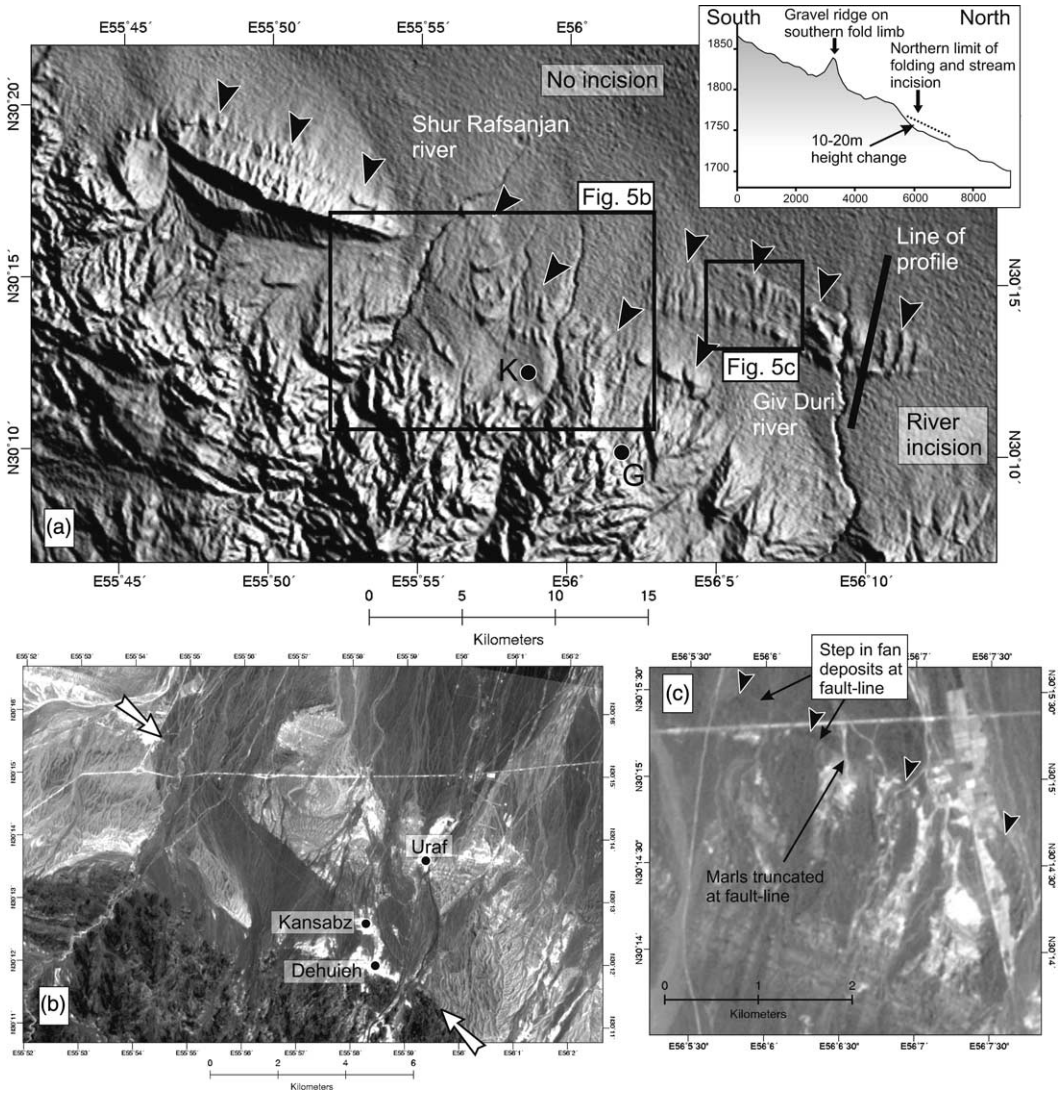

Fig. 5. (a) Shaded SRTM digital topography of the region directly south of Rafsanjan (see Fig. 2 for location). Volcanic rocks of the Kuh-e Mamzar mountains occupy the southern part of the image. The northwest–southeast Rafsanjan fault cuts through the centre of the image. Kansabz (K) and Guruieh (G) villages are situated on the fault. A series of anticlinal folds in alluvium (marked by black arrows) run along the northern side of the Rafsanjan fault trace. There is a height change of up to 10–20 m across the folds (see inset topographic profile) and incision of northward-flowing rivers ceases at the northern margin of these folds, indicating that the folds are underlain by southward-dipping thrust faults at depth (e.g. Fig. 3c). (b) ASTER satellite image (band 3n) of the Rafsanjan fault at Kansabz. The fault trace is marked by white arrows. (c) ASTER satellite image (band 3n) of folding in alluvium north of the Rafsanjan fault. Alluvial fan deposits appear to be displaced vertically along a sharp line (marked by black arrows). This line also forms an abrupt boundary between exposures of Neogene white marls and Quaternary gravels, suggesting that the thrust fault reaches the surface in this region.

likely that the two faults link together across this geological fault. However, it is difficult to determine whether the fault within the mountains is active in the Quaternary as no Quaternary sediments are present.

Southeast of the section described by Berberian (1976), the Rafsanjan fault cuts across bedrock and displaces alluvium (e.g. Fig. 4b). The fault is mapped as far east as 56°30′E, where it becomes indistinct. However, indications of faulting are again seen in ASTER satellite imagery further to the southeast, within the alluvial deposits of the Ab-e Lalehzar valley. Fig. 4c is an ASTER satellite image showing a distinct east–west scarp cutting across river terraces of the Ab-e Lalehzar river. The scarps trace westwards towards the trace of the Rafsanjan fault. The Lalehzar valley fault may be a continuation of the Rafsanjan fault (Fig. 4a).

The east–west oriented Ab-e Lalehzar valley extends for ~50 km and separates the high Kuh-e Lalehzar mountains (with peaks over 4000 m) from a lower east–west-trending range (Fig. 4a). The fault scarps described above cut obliquely across the western end of the valley floor, where the river flows northwestward. Identifying signs of active faulting further east is difficult, as unambiguous scarps are less likely to be preserved on the steep bed-rock slopes on the valley sides and fault traces along the valley floor will be rapidly degraded by fluvial erosion. It is therefore also possible that active faulting extends further east along the Ab-e Lalehzar valley.

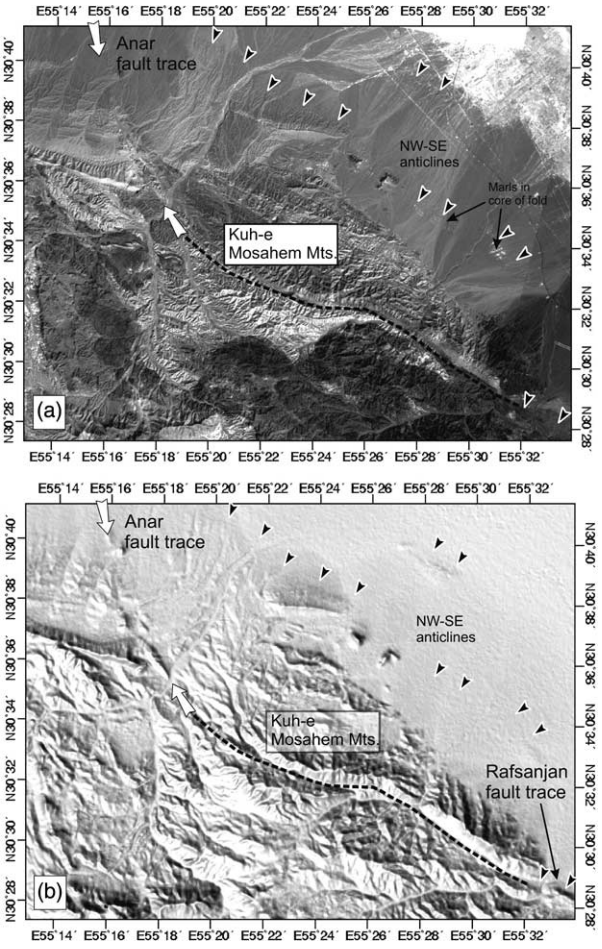

Fig. 6. (a) ASTER image (band 3n) of the Kuh-e Mosahem mountains and the southern part of the Anar fault. A series of anticlinal folds in alluvium are marked by black arrows. Light-coloured marls outcrop in the core of the folds. The Anar fault cuts through the alluvial cover of the Rafsanjan plain between the white arrows (see also Berberian, 1976; Walker and Jackson, 2004). The western end of the Rafsanjan fault cuts alluvium in the bottom right of the image. The ends of the two faults are joined by a prominent linear valley through the Kuh-e Mosahem mountains. This valley may be caused by faulting that links the Rafsanjan and Anar faults. (b) SRTM digital topography of the same region as in (a).

4.3. Thrust faulting and folding north of the Rafsanjan fault

A series of low folds are observed ~5–10 km north of the Rafsanjan fault trace (Fig. 5a). The folds are marked on published geological maps (e.g. Dimitrijevic, 1973), but neither the geology nor the structure of the folds have been described in any detail. Neogene marls are exposed in the cores of the folds. Ridges of resistant gravel deposits are preserved along the southern fold limbs (e.g. inset to Fig. 5a). However, the northern fold limbs appear to have been truncated, leaving a sharp contact between Neogene marls to the south and flat-lying gravel deposits to the north (Fig. 5c). There is a slight change in height across the fold, with a topographic profile drawn along a single, unimpeded, fan surface showing roughly 10–20 m height change between the northern (uplifted) and southern sides of the fold (inset to Fig. 5a). Northward-flowing rivers that cross the folds incise through the alluvial cover to the south of the folds, but the incision ends abruptly at the northern limit of exposure of the Neogene marls (Fig. 5a). This height change and asymmetric pattern of drainage incision indicates that the region to the south of the folding is being uplifted with respect to the northern region (e.g. Audemard, 1999; Benedetti et al., 2000; Walker et al., 2003). It is therefore likely that the folds are underlain by southward-dipping thrust faults (e.g. Section 3 and Fig. 3c), which appear to reach the Earth's surface, as shown by the sharp transition between exposures of Neogene marls and overlying gravel cover at the northern limit of the fold and also what appear to be discrete northward-facing scarps in alluvial fans at this transition (Fig. 5c).

A series of low anticlinal folds are also observed in ASTER imagery along the northern margin of the Kuh-e Mosahem mountains, where the Rafsanjan and Anar strike-slip faults appear to join (see Fig. 6). Marls within the cores of these anticlines show up as light colours in the satellite image (Fig. 6). However, there is little topographic relief across these folds in comparison with those described near Rafsanjan and those described later in this paper. The lack of topographic relief may be caused by a relatively high rate of erosion in this part of the study area, or by these folds being relict structures, with little or no activity at the present day.

4.4. Active faulting near Rafsanjan: a summary

Numerous indications of active faulting are observed in the geomorphology along the northern margin of, and within, the mountainous areas south of Rafsanjan. The previously mapped Rafsanjan fault is found to be part of a much wider zone of late Quaternary deformation, which appears to link the Sabzevaran right-lateral strike-slip fault in the southeast of the study region (Fig. 2) with a more distributed system of strike-slip faulting across wide parts of central Iran (e.g. Fig. 1c). Anticlinal folds run parallel to the main fault along its northern side. These folds are likely to overlie thrust faults at depth and may show a spatial separation of thrust and strike-slip components of motion onto separate structures. The thrusts have not previously been mapped. A possible southeastern continuation of the Rafsanjan fault system runs along the Ab-e Lalehzar river valley and Quaternary scarps are observed in the alluvial cover.

5. The Mahan folds

Folding near the town of Mahan is shown in Fig. 7. The folds trend northwest–southeast and occur along the northern margin of the Kuh-e-Jupar mountains (with elevations up to 4135 m). Abbas-Nejad and Dastanpour (1999) suggest that the folds might be related to active faulting, but no major faults are marked on the published geological maps (e.g. Sahandi, 1992; Zohrehbakhsh, 1992; Aghanabati, 1993) and no detailed information is given on either the geology or structure.

Neogene marls are exposed in the cores of the folds and appear as light colours in ASTER satellite imagery (Fig. 7). Ridges of resistant tilted gravel beds are preserved on both

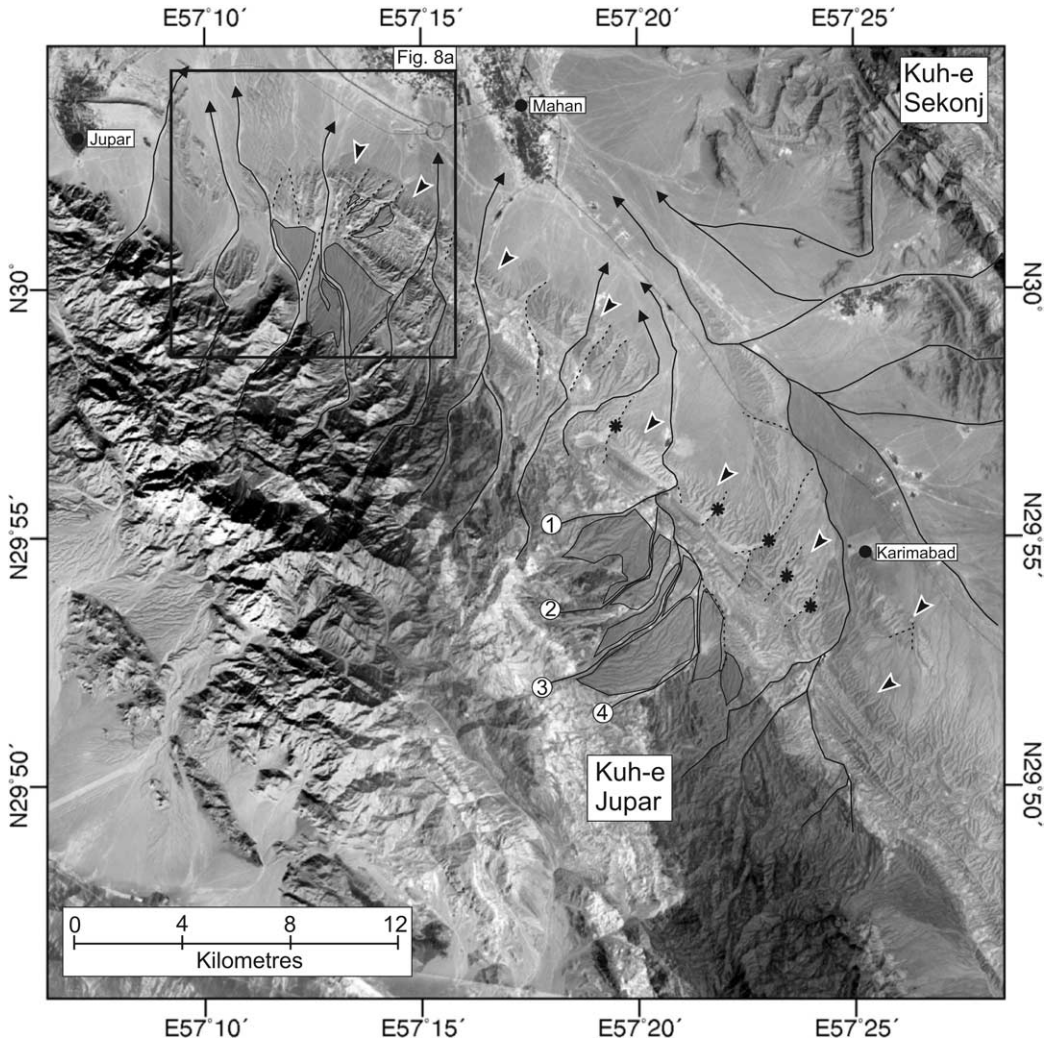

Fig. 7. ASTER image of the Mahan region. The folds occur along the northern margin of the Kuh-e-Jupar mountains and are close to the towns of Mahan and Jupar. Light-coloured marls are exposed in the cores of the folds. All fold segments have gravel ridges on both margins. Uplifted and abandoned alluvial fans are widespread to the south of the folds (marked in grey). Abandoned drainage channels are shown as dotted lines. Near Karimabad, streams 4, 3 and 2 (traced as black lines), are all deflected westwards through the fold at the outlet of stream 1. The deflection of stream 4 is ~7 km and is much larger than the apparent deflections seen further north (rivers near Jupar show a maximum westward deflection of ~2 km, see Fig. 8a). Several abandoned drainage channels are preserved as dry valleys within the fold near Karimabad (marked by black stars). These dry valleys presumably mark the original outlets of streams 4, 3 and 2. The box shows the location of Fig. 8a.

the southern and northern fold margins. Widespread remnants of alluvial fans are preserved within the anticlines (Fig. 8a). The uplifted and abandoned fan deposits are deformed where they cross the northern margin of the folds, but show a broad folding rather than a sharp step in height (Fig. 9).

Beyond the northern flank of the folds there is little indication of river incision. However, there is widespread river incision and extensive preservation of uplifted and abandoned alluvial fan systems to the south side of the folds, extending to the margin of the bed-rock mountains. The asymmetric pattern of drainage incision is similar to that seen near Rafsanjan (Fig. 5; see Section 4.3). Fig. 8a is a close-up ASTER satellite view of the western tip of the Mahan fold system. Fig. 8b is the SRTM digital topography of the same region. There is a clear change in height across the fold, which decreases westwards towards the fold tip, from ~150 to ~30 m (Fig. 8c–e). There is no variation in height in the northeastern side of the profiles (Fig. 8c–e). Northward-flowing streams are apparently deflected westwards by ~2 km as they cross the folds.

Central parts of the Mahan fold system near Karimabad (Fig. 7) have several similarities with the geomorphology seen in detail in Fig. 8, with widespread preservation of abandoned alluvial fans in the region south of the fold and an apparent westward deflection of drainage with streams 4, 3 and 2 all deflected through the outlet of stream 1. The deflected streams would originally have flowed through adjacent dry valleys (marked by black stars in Fig. 7). Stream 4 is deflected by ~7 km.

In summary, the geomorphology at Mahan shows abundant evidence of active folding. Height changes across the folds and the asymmetric pattern of river incision might indicate that the folds are underlain by southwest-dipping thrust faults. It is possible, however, that part, or all, of the height change in this example results instead from a ponding of alluvial sediment

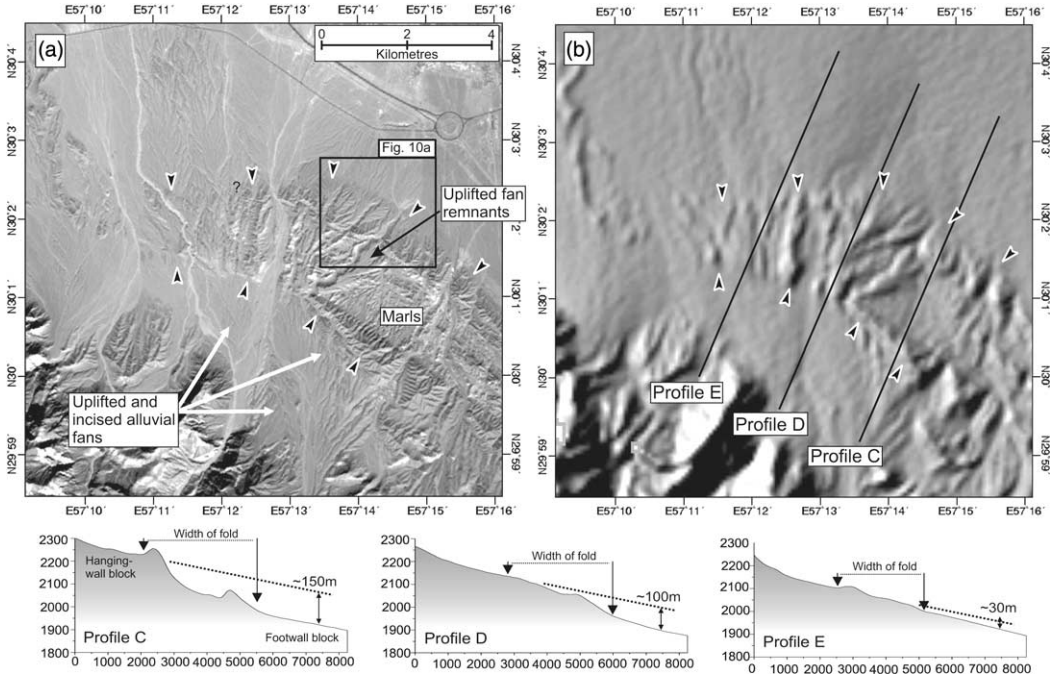

Fig. 8. (a) ASTER image of the western end of the fold at Jupar (see Fig. 7 for location). The northern and southern margins of the fold are marked by black arrows. Uplifted and abandoned alluvial fans to the south of the fold indicate possible uplift of this region with respect to the north of the fold (though in this example, the height change may result at least in part from the ponding of alluvial sediment south of the fold). Rivers appear to be deflected westwards by up to 2 km as they cross the fold. (b) SRTM topography of the same region as in (a). Profiles (c), (d) and (e) represent mean elevation along 1-km-wide swaths centred on the profile lines in (b). Scales are in metres. The gently northward-dipping slope on the hanging-wall side of the fold is projected across the fold as a dotted line. Although the angle of slope is the same in both the hanging-wall and footwall, the change in height across the fold decreases from ~150 to ~30 m westwards.

behind the fold, as the fans are developed within a rather restricted area. The preservation of both northern and southern fold limbs and the absence of discrete scarps in abandoned alluvial fans crossing the northern margin of the fold suggest that the underlying thrust fault does not reach the Earth's surface (cf. Fig. 3a) and is instead 'blind', with slip on the fault accommodated as folding within near surface sediments. Growth of the fold appears to have caused the abandonment and deflection of northward-flowing river systems.

6. The Rayen folds

In a similar fashion to the previous two examples, remote sensing imagery of the region around Rayen town was examined, to look for indications of active faulting in the local geomorphology. At Rayen, however, the remote sensing study is supported by brief field observations made in May 2001. The field observations confirm the interpretations made from satellite imagery, but also add further details, which could not be made with remote sensing on its own.

6.1. Remote sensing

Fig. 10a shows SRTM digital topography of the Rayen region. A northwest–southeast-trending band of folds runs across the centre of the image. Three individual segments are identified in the geomorphology. The town of Rayen is situated within the easternmost of the three fold segments. All three of the fold segments have a ridge composed of tilted gravels along only their southern margins (Fig. 10a). At the northern fold margins tilted Neogene marls are in sharp contact with undisturbed gravels (e.g. Fig. 10b). Remnants of uplifted, incised and abandoned alluvial fans are widespread within the folds (Fig. 10b). These fan remnants have sharp northward-facing scarps where they cross the northern, truncated limb of the fold (Fig. 10b). There is a contrast in elevation of the regional alluvial surface by ~150–200 m

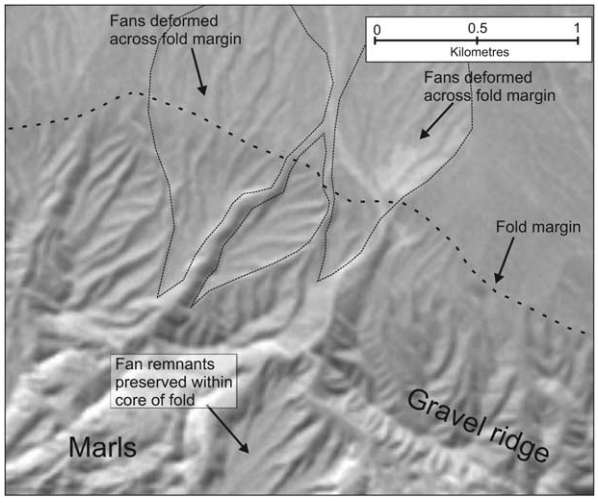

Fig. 9. Close-up ASTER image of the northern margin of the Mahan folds near Jupar (see Fig. 8a for location). Abandoned alluvial fans (outlined with thin black lines) are broadly warped across the fold margin (marked by a dotted line) and show no discrete fault scarps.

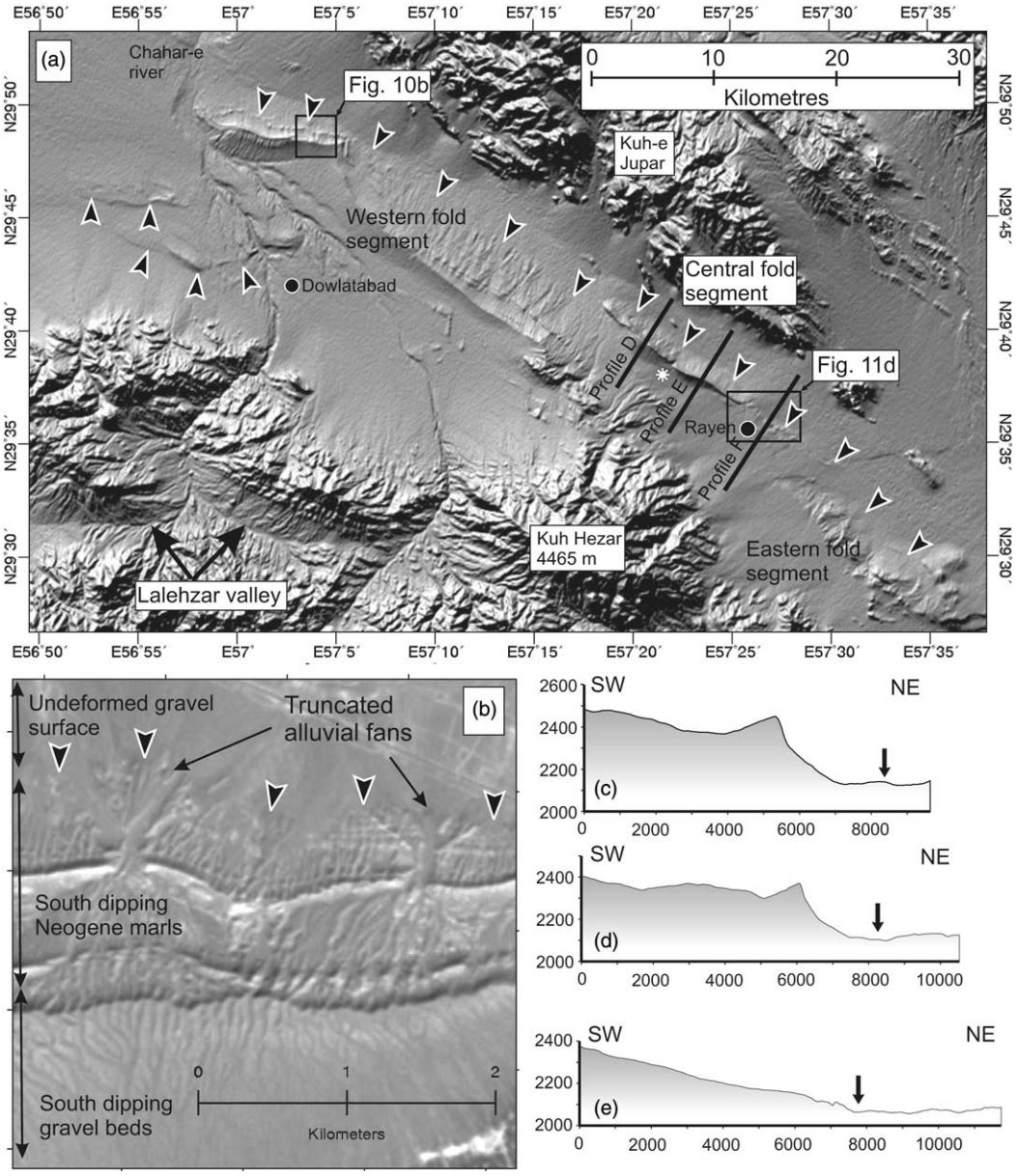

Fig. 10. (a) SRTM topography of folding at Rayen. The Kuh Hezar mountains (4465 m) occupy the lower edge of the image. Three northwest–southeast-trending fold segments are developed in alluvial cover to the northeast of the bed-rock exposure. The northern fold margins are marked by black arrows. An asymmetry of drainage incision is seen between the northwest and southeast sides of the folds, with widespread incision of drainage in the region around Dowlatabad. A wind-gap through the central fold segment is marked by a white star. Folding at Rayen itself has less topographic expression. The black lines mark the positions of the three topographic sections. (b) ASTER image (band 3n) showing a small part of the western fold segment at Rayen (marked by a box in (a)). Obvious scarps in alluvial fan deposits and a sharp contact between outcrops of Neogene marl beds and undeformed gravel deposits to the north is strong evidence for the fault reaching the surface in this region. (c) Topographic section through the central Rayen fold segment. Up to 200 m of topographic relief is seen across the fold. The black arrow marks the northern limit of folding. (d) Another section through the central Rayen fold segment. Again, a topographic contrast of 150–200 m is seen across the fold. (e) Topographic profile through the eastern fold segment at Rayen. The height contrast across the fold is much less than in the other sections and yet the limit of folding can still be seen (marked by black arrow).

across the ~15-km-long fold central fold segment (see topographic sections; Fig. 10c and d), though this elevation change may result in part from ponding of alluvial material behind the back-limb gravel ridge (e.g. Fig. 10a). The eastern fold segment at Rayen town also has an elevation change of ~50 m of the regional northward directed slope (Fig. 10e). The elevation change across the eastern fold segment occurs immediately north of the town and is unlikely to result from localised ponding of alluvial sediment, as it occurs across a low relief plain, with little in the way of obstructing topography.

The present-day drainage is directed northeast. The white star in Fig. 10a represents an abandoned and uplifted drainage channel, or ‘wind-gap’, for streams that are now deflected around the ends of the central fold segment. Drainage adjacent to the western fold segment is deflected westward for more than 30 km, to flow round the end of the anticline as the Chahar-e river (Fig. 10a).

As in the previous examples, the observations described above show that active folding occurs in the Rayen region. Elevation changes of at least 50 m across the folds indicate the presence of underlying thrust faults, which, from the truncation of the northern fold limb and the discrete northward-facing scarps developed in alluvial fans crossing the northern fold margin, is likely to reach the Earth's surface.

6.2. Additional field observations

Fig. 11a is a view looking along the central segment of the Rayen fold system from its eastern end. Features identified in the remote sensing imagery such as uplifted alluvial fans, a gravel ridge along the southern fold limb and a 'wind-gap' through the ridge can all be seen. In the northern limb of the fold, discontinuous southward-dipping faults are developed in steep southward-dipping volcaniclastic rocks that outcrop through the abandoned alluvial fans (Fig. 11b). These faults trend parallel to the axis of the fold and appear to be minor normal faults, possibly related to extension along the axis of a growing fold (similar to structures developed, for instance, during the 1994 Sefidabeh earthquake sequence in Sistan province of eastern Iran; Berberian et al., 2000). The slip-vector measured from striations on the fault-plane (Fig. 11c) indicates a strike-slip component of motion.

Fig. 11d is a close-up ASTER image of Rayen town (see Fig. 10a for location). Black arrows point to a line of uplifted light-coloured rocks along the northern margin of the fold.

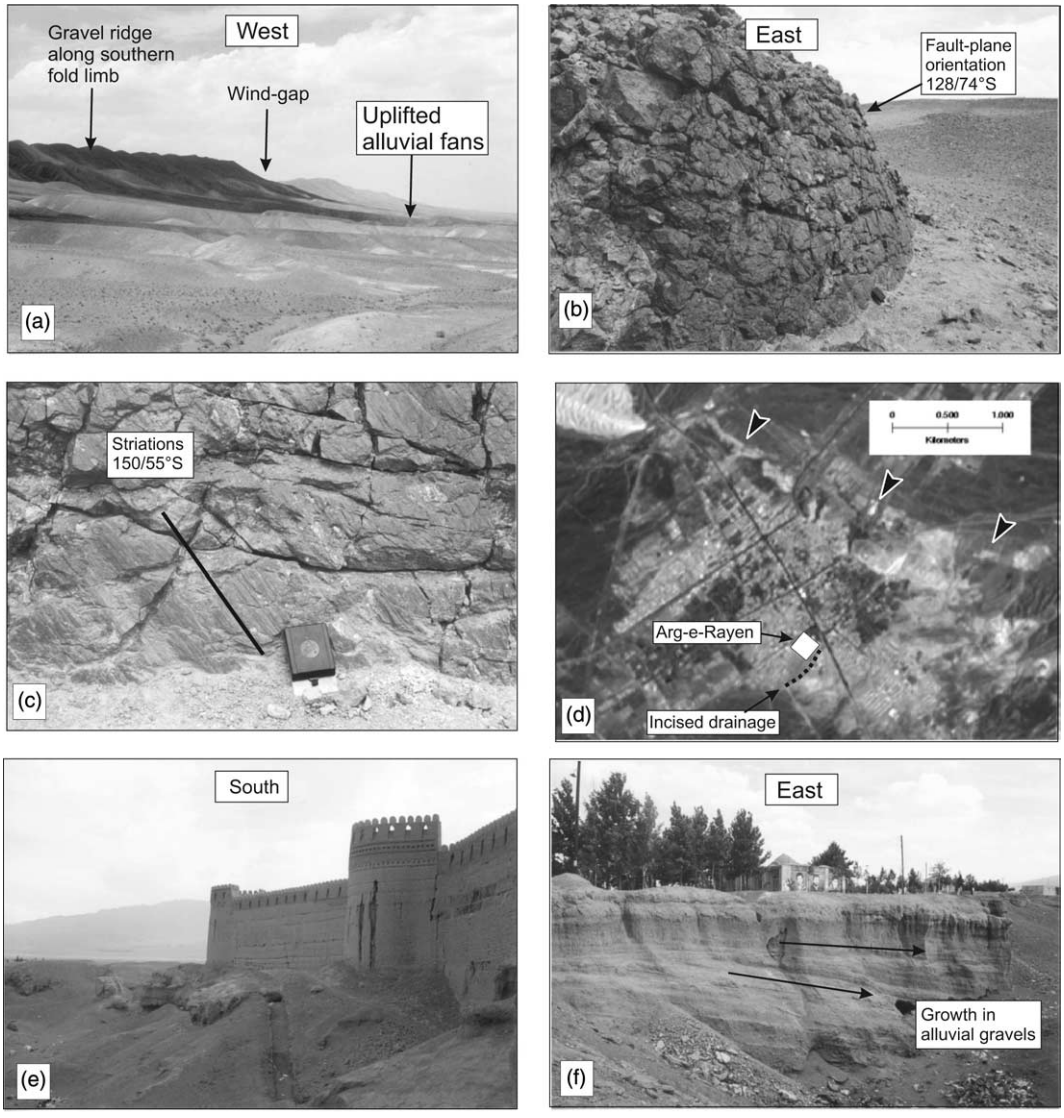

Fig. 11. (a) View westwards along the central fold segment west of Rayen. There is a prominent wind-gap in the centre of the view. The interior of the fold has been stripped away by erosion, but extensive remnants of uplifted fans are preserved. (b) Normal faulting in volcaniclastic bed-rock within the Rayen folds at 29°37′.50N 57°25′.92E. The fault-plane trends parallel to the fold axis (~130°). (c) Close-up view of the striated fault surface shown in (b). The striations indicate an oblique slip-vector. (d) Close-up ASTER image of Rayen town. The northern limit of folding is marked by black arrows. The Arg-e-Rayen and incised drainage shown in (e) and (f) are highlighted. (e) The Arg-e-Rayen (Citadel of Rayen) at 29°36′.00N 57°26′.65E. The castle is built on a high alluvial surface overlooking the town with incised drainage channels around its edges as natural defences. (f) Looking eastwards from the Arg-e-Rayen into the wall of an incised drainage channel. Southward-dipping gravels are seen. Overlying gravels dip more gently and truncate underlying beds, showing growth of the fold (e.g. Fig. 3b).

There are examples of river incision and of preserved remnants of uplifted alluvial fans within the town. The old citadel (the Arg-e-Rayen) is built on the edge of an uplifted and incised fan at the southern end of town (Fig. 11d and e). Incised rivers provide natural defences around the castle (Fig. 11d–f). The gravels within the uplifted fan dip gently southwards (Fig. 11f), showing that the castle is situated on the southern limb of the fold. Unconformable relationships between younger over-lying gravels and underlying, more steeply-dipping gravels are seen in exposures next adjacent to the castle (Fig. 11f). Unconformable relationships such as these represent deposition of sediment during growth of the fold (e.g. Fig. 3b; Burbank et al., 1996) and are commonly observed in regions of active folding, such as at Tabas and Ferdows in eastern Iran (Walker et al., 2003).

7. Discussion

The observations in this paper are used to produce a detailed map of active faulting in southern Kerman province. It appears that late Quaternary strike-slip and thrust faulting is widespread within the region, a result that would not be expected from published GPS velocities alone (e.g. Vernant et al., 2004a,b) or the distribution of historical and recent seismicity (e.g. Ambraseys and Melville, 1982; Berberian and Yeats, 1999). Walker and Jackson (2004) suggest that intense faulting in southern Kerman province may be related to present-day activity on the Deh Shir and Anar strike-slip faults within central parts of Iran (Fig. 1), which they suggest may result from these strike-slip faults accommodating small amounts of Arabia–Eurasia shortening by rotating anticlockwise about a vertical axis, resulting in diffuse deformation within the fault-bounded blocks. Whether or not this is the case, the diffuse band of faulting described in this paper does appear to link the Sabzevaran and Anar strike-slip faults (Figs. 1 and 2) and, as such, does indicate that the faults are important in the transfer of tectonic strain across the region by distributing a part of the right-lateral shear between the Zagros mountains and the Makran across right-lateral fault systems within central parts of Iran.

The faults appear to be active and may therefore have the potential to generate large earthquakes. The potential for destructive earthquakes in this part of Iran is shown by the 1923 Lalehzar earthquake (Berberian, 1976; Ambraseys and Melville, 1982). The Lalehzar earthquake occurred close to the Rafsanjan fault, but we cannot assign the event to this fault with any degree of certainty as it is possible that other active structures exist within the region. Very few historical or instrumental earthquakes have been recorded elsewhere in the study area. The apparent lack of historical seismic activity may be real, as there are several ancient towns in the region for which records of earthquake damage might be expected (Ambraseys and Melville, 1982). In addition, we know that the rates of deformation across central parts of Iran are very low (e.g. Vernant et al., 2004a,b) and repeat times between earthquakes on individual faults may be several thousand years (e.g. Berberian and Yeats, 1999). Remote sensing observations alone cannot show the potential for earthquakes to occur on an individual fault segment. However, given that the fault segments identified in this study are typically at least 10–15 km in length, if they do fail in earthquakes, they could generate destructive events with magnitudes of >6 (Scholz, 1982). Palaeoseismic investigations and age estimates on remnants of Quaternary fans uplifted and displaced by the active faults would provide information on the likely size and repeat time of earthquakes on individual faults identified in this study.

The present-day rates of slip across the faults in the study region must be low (e.g. Vernant et al., 2004a). The faults are, however, very well exposed, show clear evidence of late Quaternary movement and can easily be identified in satellite imagery. The types of observation used in this paper are not new and have been established by previous studies that have exploited the link between slip on faults (typically in earthquakes) with long-term fault movements and the development of landscapes (previous studies within Iran include, for instance, Berberian et al. (2000) and Walker et al. (2003, 2005)). However, the ability to apply the results of such studies over very large areas relies on the availability of remote sensing data such as the SRTM digital topographic dataset and 15 m ASTER satellite imagery. It is therefore the increasing availability of global remote sensing data that make reconnaissance studies of active faulting feasible.

8. Conclusion

A conclusion of this paper is that widespread active faulting is present in a part of central Iran that is often referred to as a rigid block within the Arabia–Eurasia collision and therefore assumed not to be deforming. The faulting identified in this paper is hence important for descriptions of the tectonics of eastern Iran, as deformation in the region must play a role in the overall deformation of eastern Iran that might otherwise be overlooked. Although remote sensing observations such as those presented here cannot show the potential for earthquakes on individual structures, the identification and mapping of active faults is a useful guide for future, more detailed studies. It is important to remember that fault slip at low rates (<2 mm/yr) can still produce occasional devastating earthquakes. The 1923 Rafsanjan earthquake is one such example. The 2003 Bam earthquake is another (e.g. Talebian et al., 2004), as no previous events are recorded at Bam, despite its long recorded history (e.g. Talebian et al., 2004; Jackson et al., in review). Remote sensing studies can provide a valuable first step in the identification and analysis of active faulting in actively deforming regions.

Acknowledgements

I thank the Geological Survey of Iran for their kind support, which has allowed me to work in Iran over several years. L.A. Ramsey helped to generate the topographic profiles. Population figures were provided by M. Talebian. M. Rezaeian helped with translation from Persian. J. Jackson provided helpful comments on an early draft of the paper. The final paper was

improved by helpful reviews from Philippe Vernant and an anonymous reviewer. ASTER satellite imagery and SRTM topography are courtesy of NASA. RTW is supported by a NERC fellowship and by the NERC Centre for the Observation and Modelling of Earthquakes and Tectonics (COMET). Part of the work in this paper was undertaken at Cambridge University as part of a PhD thesis.

References

Abbas-Nejad, A., Dastanpour, M., 1999. Earthquakes and Seismicity of Kerman Region. Mascan and Shahrsazi Organization of Kerman (in Persian).

Aghanabati, A., 1993. Geological quadrangle map of Iran, 1:250,000 scale. Sheet No. J11. Geological Survey of Iran, Tehran, Iran.

Ambraseys, N.N., Melville, C.P., 1982. A History of Persian Earthquakes. Cambridge University Press, Cambridge, UK.

Ambraseys, N.N., Tchalenko, J.S., 1969. The Dasht-e-Bayaz (Iran) earthquake of August 31, 1968: A field report. Bulletin of the Seismological Society of America 59, 1751–1792.

Audemard, F.A., 1999. Morpho-structural expression of active thrust fault systems in the humid tropical foothills of Colombia and Venezuela. Zeitschrift für Geomorphologie 118, 227–244.

Benedetti, L., Tapponnier, P., King, G.C.P., Meyer, B., Manighetti, I., 2000. Growth folding and active thrusting in the Montello region, northern Italy. Journal of Geophysical Research 105, 739–766.

Berberian, M., 1976. Contribution to the seismotectonics of Iran (Part II). Geological Survey of Iran, Report No. 39.

Berberian, M., Yeats, R.S., 1999. Patterns of Historical Earthquake Rupture in the Iranian Plateau, Bulletin of the Seismological Society of America, 89, 120–139.

Berberian, M., Jackson, J.A., Qorashi, M., Talebian, M., Khatib, M.M., Priestley, K., 2000. The 1994 Sefidabeh earthquakes in eastern Iran: blind thrusting and bedding-plane slip on a growing anticline, and active tectonics of the Sistan suture zone. Geophysical Journal International 142, 283–299.

Berberian, M., Baker, C., Fielding, E., Jackson, J.A., Parsons, B.E., Priestley, K., Qorashi, M., Talebian, M., Walker, R., Wright, T.J., 2001. The March 14 1998 Fandoqa earthquake (Mw 6.6) in Kerman province, SE Iran: re-rupture of the 1981 Sirch earthquake fault, triggering of slip on adjacent thrusts, and the active tectonics of the Gowk fault zone. Geophysical Journal International 146, 371–398.

Boudiaf, A., Ritz, J.-F., Philip, H., 1998. Drainage diversions as evidence of propagating active faults: example of the El Asnam and Thenia faults, Algeria. Terra Nova 10, 236–244.

Brown, E.T., Bourles, D.L., Raisbeck, G.M., Yiou, F., 1998. Estimation of slip rates in the southern Tien Shan using cosmic ray exposure dates of abandoned alluvial fans. Geological Society of America Bulletin 110, 377–386.

Burbank, D., Meigs, A., Brozovic, N., 1996. Interactions of growing folds and coeval depositional systems. Basin Research 8, 199–223.

Champel, B., van der Beek, P., Mugnier, J.-L., Leturmy, P., 2002. Growth and lateral propagation of fault-related folds in the Siwaliks of western Nepal: rates, mechanisms, and geomorphic signature. Journal of Geophysical Research 107 (B6). doi:10.1029/2001JB000578.

Cowie, P.A., Scholz, C.H., 1992. Growth of faults by accumulation of seismic slip. Journal of Geophysical Research 97, 11,085–11,095.

Dimitrijevic, M.D., 1973. Geology of Kerman Region. Institute for Geological and Mining Exploration and Investigation of Nuclear and Other Mineral Raw Materials. Report no. Yu/52, 1973, Belgrade.

Engdahl, E.R., van der Hilst, R., Buland, R., 1998. Global teleseismic earthquake relocation with improved travel times and procedures for depth determination, Bulletin of the Seismological Society of America, 88, 722–743.

Fattahi, M., Walker, R., Hollingsworth, J., Bahroudi, A., Talebian, M., Armitage, S., Stokes, S., in review. Holocene slip-rate on the Sabzevar thrust fault, NE Iran, determined using optically-stimulated luminescence (OSL). Earth and Planetary Science Letters.

Fielding, E.J., Wright, T.J., Muller, J., Parsons, B.E., Walker, R., 2004. Aseismic deformation of a fold-and-thrust belt imaged by synthetic aperture radar interferometry near Shahdad, southeast Iran. Geology 32, 577–580.

Hollingsworth, J., Jackson, J., Walker, R., Gheitanchi, M.R., Bolourchi, M.J., in press. Strike-slip faulting, rotation, and along-strike elongation in the Kopeh Dagh mountains, NE Iran. Geophysical Journal International, in press.

Jackson, J., Norris, R., Youngson, J., 1996. The structural evolution of active fault and fold systems in central Otago, New Zealand: evidence revealed by drainage patterns. Journal of Structural Geology 18, 217–234.

Jackson, J., Fielding, E., Funning, G., Ghorashi, M., Hatzfeld, D., Nazari, H., Parsons, B., Priestley, K., Rosen, P., Talebian, M., Tatar, M., Walker, R., Wright, T., in review. Seismotectonic aspects of the 26 December 2003 Bam, Iran, earthquake. Geophysical Journal International.

Keller, E.A., Zepeda, R.L., Rockwell, T.K., Ku, T.L., Dinklage, W.S., 1998. Active tectonics at Wheeler Ridge, southern San Joaquin Valley, California. Geological Society of America Bulletin 110, 298–310.

Keller, E.A., Gurrola, L., Tierney, T.E., 1999. Geomorphic criteria to determine direction of lateral propagation of reverse faulting and folding. Geology 27, 515–518.

Lettis, W.R., Wells, D.L., Baldwin, J.N., 1997. Empirical observations regarding reverse earthquakes, blind thrust faults, and Quaternary deformation: are blind thrust faults truly blind? Bulletin of the Seismological Society of America 87, 1171–1198.

McClusky, S., Reilinger, R., Mahmoud, S., Ben Sari, D., Tealeb, A., 2003. GPS constraints on Africa (Nubia) and Arabia plate motions. Geophysical Journal International, 155, 126–138.

Pan, B., Burbank, D., Wang, Y., Wu, G., Li, J., Guan, Q., 2003. A 900 k.y. record of strath terrace formation during glacial–interglacial transitions in northwest China. Geology 31, 957–960.

Regard, V., Bellier, O., Thomas, J.-C., Bourles, D., Bonnet, S., Abbassa, M.R., Braucher, R., Mercier, J., Shabanian, E., Soleymani, Sh., Feghhi, Kh., 2005. Cumulative right-lateral fault slip-rate across the Zagros–Makran transfer zone: role of the Minab–Zendan fault system in accommodating Arabia–Eurasia convergence in southeast Iran. Geophysical Journal International 162, 177–203.

Sahandi, M.R., 1992. Geological quadrangle map of Iran, 1:250,000 scale. Sheet No. J10 (Kerman). Geological Survey of Iran, Tehran, Iran.

Scholz, C.H., 1982. Scaling laws for large earthquakes: consequences for physical models. Bulletin of the Seismological Society of America 72, 1–14.

Sella, G.F., Dixon, T.H., Mao, A., 2002. REVEL: a model for recent plate velocities from space geodesy. Journal of Geophysical Research 107. doi:10.1029/2000JB000033.

Stein, R., King, G.C.P., 1984. Seismic potential revealed by surface folding: the 1983 Coalinga, California, earthquake. Science 224, 869–872.

Stein, R., Yeats, R.S., 1989. Hidden earthquakes. Scientific American 260, 48–57.

Stocklin, J., 1968. Structural history and tectonics of Iran: a review, Bulletin of the American Association of Petroleum Geologists, 52, 1229–1258.

Talebian, M., Fielding, E.J., Funning, G.J., Jackson, J., Nazari, H., Parsons, B., Priestley, K., Qorashi, M., Rosen, P.A., Walker, R., Wright, T.J., 2004. The 2003 Bam (Iran) earthquake—rupture of a blind strike-slip fault. Geophysical Research Letters 31, L11611. doi:10.1029/2004GL020058.

Van der Beek, P., Champel, B., Mugnier, J.-L., 2002. Control of detachment dip on drainage development in regions of active fault-propagation folding. Geology 30, 471–474.

Van der Woerd, J., Tapponnier, P., Ryerson, F.J., Meriaux, A.-S., Meyer, B., Gaudemer, Y., Finkel, R.C., Caffee, M.W., Guoguang, Z., Zhiqin, X., 2002. Uniform postglacial slip-rate along the central 600 km of the Kunlun fault

(Tibet), from ^{26}Al, ^{10}Be, and ^{14}C dating of riser offsets, and climatic origin of the regional morphology. Geophysical Journal International 148, 356–388.

Vernant, Ph., Nilfroushan, F., Hatzfeld, D., Abbassi, M.R., Vigny, C., Masson, F., Nanakali, H., Martinod, J., Ashtiani, A., Bayer, R., Tavakoli, F., Chery, J., 2004a. Contemporary crustal deformation and plate kinematics in Middle East constrained by GPS measurements in Iran and northern Oman. Geophysical Journal International 157, 381–398.

Vernant, Ph., Nilfroushan, F., Chery, J., Bayer, R., Djamour, Y., Masson, F., Ritz, J.-F., Sedighi, M., Tavakoli, F., 2004b. Deciphering oblique shortening of central Alborz in Iran using geodetic data. Earth and Planetary Science Letters 223, 177–185.

Walker, R., Jackson, J., 2002. Offset and evolution of the Gowk fault, S.E. Iran: a major intra-continental strike-slip system. Journal of Structural Geology 24, 1677–1698.

Walker, R., Jackson, J., 2004. Active tectonics and late Cenozoic strain distribution in central and eastern Iran. Tectonics 23, TC5010. doi:10.1029/2003TC001529.

Walker, R., Jackson, J., Baker, C., 2003. Thrust faulting in eastern Iran: source parameters and surface deformation of the 1978 Tabas and 1968 Ferdows earthquake sequences. Geophysical Journal International 152, 749–765.

Walker, R., Jackson, J., Baker, C., 2004. Active faulting and seismicity of the Dasht-e-Bayaz region, eastern Iran. Geophysical Journal International, 157, 265–282.

Walker, R.T., Bergman, E., Jackson, J., Ghorashi, M., Talebian, M., 2005. The 2002 June 22 Changureh (Avaj) earthquake in Qazvin province, northwest Iran: epicentral relocation, source parameters, surface deformation and geomorphology. Geophysical Journal International 160, 707–720.

Zohrehbakhsh, A., 1992. Geological quadrangle map of Iran, 1:250,000 scale. Sheet No. I10 (Rafsanjan). Geological Survey of Iran, Tehran, Iran.